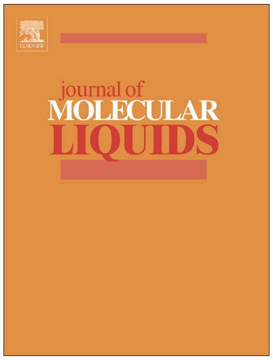

Removal of nitrate from aqueous solution using modified granular activated carbon

Mahmoud Mazarji, Behnoush Aminzadeh, Majid Baghdadi, Amit Bhatnagar

PII: S0167-7322(17)30304-5
DOI: doi: 10.1016/j.molliq.2017.03.004
Reference: MOLLIQ 7037

To appear in: *Journal of Molecular Liquids*

Received date: 22 January 2017
Revised date: 28 February 2017
Accepted date: 1 March 2017

Please cite this article as: Mahmoud Mazarji, Behnoush Aminzadeh, Majid Baghdadi, Amit Bhatnagar , Removal of nitrate from aqueous solution using modified granular activated carbon. The address for the corresponding author was captured as affiliation for all authors. Please check if appropriate. Molliq(2017), doi: 10.1016/j.molliq.2017.03.004

Removal of nitrate from aqueous solution using modified granular activated carbon

Mahmoud Mazarji [1,*], Behnoush Aminzadeh [1], Majid Baghdadi [1], Amit Bhatnagar [2,*]

[1] *Department of Environmental Engineering, Graduate Faculty of Environment,*
University of Tehran, P.O. Box: 1417853111, Tehran, Iran

[2] *Department of Environmental and Biological Sciences, University of Eastern Finland,*
P.O. Box 1627, FI-70211 Kuopio, Finland

*Corresponding authors: Emails: mazarji@ut.ac.ir; amit.bhatnagar@uef.fi

Abstract

In this study, a commercial granular activated carbon was modified with sodium hydroxide followed by a cationic surfactant to increase its efficiency for nitrate removal from water. Physicochemical properties of untreated activated carbon and treated activated carbons were characterized in the terms of FTIR spectroscopy, N_2 adsorption-desorption, and SEM analyses. The surface properties of ACs were determined by N_2-adsorption isotherm data and modeled with several mathematical models. The results showed that the combination of two treatments could improve the nitrate removal efficiency, which is mainly attributed to the modification by cationic surfactant, while the porous volume and specific surface area did not seem to play an important role in the nitrate uptake. In batch experiments, the influence of several operating parameters on the nitrate adsorption capacity was investigated including solution pH, adsorbent dosage, contact time, initial nitrate concentration, temperature and competing ions. Small continuous column test was performed to investigate the feasibility of using each adsorbent. Results of this study suggest that using two-step treatment can be a promising method to enhance the efficiency of activated carbon for nitrate removal from water.

Keywords: Adsorption; Nitrate removal; Cationic surfactant treatment; Modified activated carbon; Alkaline treatment.

1 Introduction

Increasing nitrate concentrations in groundwater in various countries have been observed in the recent past [1–5]. Concentrations of $NO_3^- - N$ in groundwater have been increasing by 1–3 mgL^{-1} annually during the last two decades throughout the world [6]. This phenomenon mainly occurs due to the increased agricultural activity which is necessary for enhanced food production and also due to the industrial activity [7,8]. Drinking water, high in nitrate concentration, can potentially cause health problems such as blue baby syndrome (methemoglobinemia) in infants [9] and increase the incidence rates of stomach cancer, colorectal cancer and non-Hydgkin's Lymphoma in adults [10]. Therefore, the World Health Organization (WHO) has set the maximum contaminant level (MCL) of 50 mgL^{-1} nitrate in drinking water [11], while the US Environmental Protection Agency (US EPA) has stipulated 44.2 mgL^{-1} nitrate [12].

Due to the high solubility and stability, this ion has a low tendency to be removed by using conventional water treatment technologies such as lime softening and filtration [3]. Several physicochemical and biological methods have been applied to remove excessive nitrate from water including adsorption, ion exchange, reverse osmosis, electrodialysis, and denitrification [9]. Among all these techniques, adsorption, considering from economy and efficiency points of view, is a practical process due to convenience, ease of operation and simplicity of design, although it requires highly efficient adsorbents [13–15]. Adsorption by activated carbons (ACs) in the field of water treatment has become one reliable method and proven to be very efficient in the removal of a wide variety of contaminants [16,17]. Nevertheless, the effectiveness of adsorption by ACs in the forms of powder or granular for nitrate uptake is quite poor [15] and only few studies have reported the adsorption of NO_3^- using ACs [18].

To overcome this limitation, research is being directed towards post-treatment methods involving modifications in physicochemical properties of ACs including acid treatments [5,19], impregnation of metal and metal oxides [14,20], cationic surfactants [21], thermal [17], outgassing and ammonia gas treatment [4], and urea post-treatment [17]. However, up to now, no investigations have been carried out on utilizing alkaline treatment with sodium hydroxide as a treatment for commercially available ACs in case of nitrate uptake.

Generally, these modifications can significantly alter the physical properties of activated carbon, such as surface area and pore volume and also chemical properties by introducing new surface functional groups [22]. Studies have shown that surface chemistry rather than structural properties seems to play a key role in the nitrate uptake [5,13,17].

In this study, a commercial granular activated carbon (AC) was treated with sodium hydroxide followed by a cationic surfactant (cetyl trimethyl ammonium bromide) to increase its efficiency for nitrate removal. The specific objectives of the present study were to: (1) investigate the effect of the alkaline treatment on the texture properties of the commercially activated carbon, (2) evaluate the combination of two treatments on adsorption of nitrate in batch and small continuous column experiments. Various isotherms and kinetic models were applied to fit the experimental data. In addition, the influence of several operating parameters on the adsorption of nitrate on ACs was also investigated as a function of pH, adsorbent dosage, contact time, initial nitrate concentration, temperature and competitive ions. The results are presented and discussed in this study.

2 Materials and Methods

2.1 Materials

Commercial activated carbon (CAC) used in this study was a granular type (30–40 mesh) produced by the vapor activation of coconut shell, purchased from Kimia Carbon Co., Arak, Iran. The cationic surfactant used in this study was $C_{13}H_{42}NBr$ (Cetyl trimethyl ammonium bromide (CTAB)), obtained from Central Drug House (CDH) with 99% purity, and used as received. The critical micelle concentration (CMC) of CTAB was reported as 0.92 mM 25 °C [23]. All other chemicals were of analytical grade and purchased from Merck (Germany). A stock solution of nitrate (1000 mgL^{-1}) was used to prepare the desired concentration of the nitrate solutions by serial dilution of the stock solution.

2.2 Modification of activated carbon

Prior to use, CAC was washed repeatedly with hot distilled water to remove soluble impurities, and dried overnight in an oven at 60 °C. The washed CAC was referred to as AC and transferred to a desiccator until use. Five g of NaOH was well mixed by stirring, with 100 mL of an aqueous solution constantly for 10 min. Ten g of AC was added to the slurry. The mixing was performed at 75 °C for 7 h. The product was subsequently washed with 0.5 M HCl and then several times with distilled water until complete removal of the salts. The resulting product was allowed to dry at 60 °C in an oven for overnight. The AC obtained in this process was denoted as AC-1. 0.1677 g of CTAB was added to 1 L solution (at pH=7), which corresponds to the 0.5 critical micelle concentration (CMC). Above the CMC, the surfactant forms micelles that remain in the bulk zone, hence a concentration of 0.5 CMC was selected to maximize the amount of surfactant adsorbed onto AC [24]. The solution was kept stirring to dissolve the precipitates completely. Two grams AC-1 was added to it, and then the reaction mixture was stirred for 5 h at room temperature. After modification, the particles were washed several times with distilled water and dried at 60 °C in an oven for 24 h. This adsorbent is termed as AC-2.

2.3 Characterization of adsorbents

The adsorbents were analyzed with Fourier transform infrared (FTIR) spectroscopy (Perkin-Elmer model Spectrum Two). The texture properties of the activated carbons were determined from the N_2 adsorption−desorption isotherms at 77 K using a BELsorp-mini II, Japan instrument. Appropriate mathematical models were used to examine the adsorption isotherms of ACs including: (i) BET equation for total surface area, (ii) Dubinin–Radushkevich (D-R) equation for micropore volume, (iii) nitrogen uptake at the relative pressure of 0.98 for total pore volume, (iv) the deduction of micropore volume from total pore volume for mesopore volume, and (v) Barrett–Joyner–Halenda (BJH) method for calculating pore size distribution. Scanning electron microscope (SEM HITACHI S-4160, Japan) was also used to study the surface morphology of the adsorbents.

2.4 Batch adsorption studies

In order to examine the effectiveness of each modificiation step in the removal of nitrate, batch experiments were conducted. A fixed amount of each adsorbent (0.2 g) in tubes containing 50 mL of a nitrate solution (40 mgL^{-1}) was kept with a speed of 200 rpm at initial pH of about 7. After equilibrium, samples were filtered using 0.45 µm filters (Whatman, USA) and the residual nitrate concentrations in solution were determined by a UV-visible spectrophotometer (HACH, DR 5000, USA) at a wavelength of 500 nm using the cadmium reduction method with the reagent NitraVer from HACH (cadmium reduction method, HACH, 8039). All experiments were performed at room temperature (25 °C). Nitrate removal percentage was calculated as follows:

$$Removal\ (\%) = \frac{(C_0 - C_e)}{C_0} \times 100 \tag{1}$$

where C_0 and C_e are the initial and equilibrium nitrate concentrations in the solutions, respectively. Each experiment was triplicated to determine the reproducibility of the measurements and the average values are reported.

2.4.1 *Effect of solution pH*

The effect of pH on the nitrate removal was investigated for AC-2 due to its excellent performance for the removal of nitrate. The pH of nitrate solutions (40 mgL^{-1}) was adjusted to different values (3-11) by diluted NaOH and HCl solution. For every experiment, 50 mL of the pH adjusted solution and 0.2 g the adsorbent were mixed and agitated for 120 min. The amount of nitrate adsorbed per unit weight of adsorbent (q_e in mg g^{-1}) was calculated as follows:

$$q_e = \left(\frac{C_0 - C_e}{m}\right)V \tag{2}$$

where C_0 and C_e (mgL^{-1}) are the initial and equilibrium concentrations of nitrate ions in solutions, m is the mass of the adsorbent (g) and V is volume of the solution (L).

2.4.2 *Effect of adsorbent dosage*

The effect of the adsorbent dosage on nitrate removal was determined by containing 50 mL of solution with an initial nitrate concentration of 40 mgL^{-1} using the jar test at the optimum pH. Different amounts of the adsorbent (0.05-0.5 g) were studied. After the equilibrium time, the concentration of nitrate in the supernatant solution was analyzed.

2.4.3 *Adsorption kinetic studies*

Adsorption kinetic study was conducted by adding 4 g of the adsorbent into glass beaker containing 1 L nitrate solution in two different concentrations (40 and 80 mgL^{-1}) to determine the minimum time required for adsorption to reach equilibrium at the optimum pH. At selected time intervals, 10 mL samples were extracted to determine the concentration of nitrate. The amount of nitrate adsorbed at time t, q_t (mgg^{-1}) was calculated by:

$$q_t = \left(\frac{C_0 - C_t}{m}\right) V \tag{3}$$

where C_t (mgL^{-1}) is the concentration of nitrate ions at indicated time, m is the mass of the adsorbent (g) and V is volume of the solution (L).

The kinetic adsorption data can be exploited to evaluate the order and the rate constant of adsorption [25]. To investigate the mechanism of adsorption and potential rate controlling steps such as chemical reaction, diffusion control, and mass transport processes, three kinetic models, namely pseudo-first-order (Eq. (4)) [26], pseudo-second-order (Eq. (5)) [27], and intra-particle diffusion (Eq. (6)) [28] kinetic models were used to test the experimental data. The non-linear forms of these models are given below:

$$q_t = q_e(1 - e^{-k_1 t}) \tag{4}$$

$$q_t = \frac{{q_e}^2 k_2 t}{1 + q_e k_2 t} \tag{5}$$

$$q_t = k_{id} t^{1/2} + \theta \tag{6}$$

where q_e is the amount of adsorbed nitrate on the AC-2 (mgg^{-1}) at equilibrium time, k_1 is the Lagergren’s rate constant of adsorption (min^{-1}); k_2 is the equilibrium rate constant of pseudo-second-order (gmg^{-1} min^{-1}); k_{id} is the intra-particle diffusion rate constant (mgg^{-1}min$^{-1/2}$), and θ (mgg^{-1}) is the intercept.

2.4.4 Adsorption isotherm studies

Adsorption isotherm experiments were carried out by varying the concentration of nitrate solution from 40-200 mgL^{-1} under the same conditions as the adsorption kinetics experiments. To provide an insight into the surface properties and as well as the degree of affinity of the adsorbent, the adsorption data was fitted with four adsorption isotherms, namely, the Langmuir (Eq. (7)) [29], Freundlich (Eq. (8)) [30], Sips (Eq. (9)) [31] and Redlich-Peterson (Eq. (10)) [32] equilibrium isotherms using the non-linear forms of these models:

$$q_e = \frac{bC_e q_m}{1 + bC_e} \tag{7}$$

$$q_e = K_f C_e^{\frac{1}{n}} \tag{8}$$

$$q_e = \frac{q_m K_s C_e^{\frac{1}{n}}}{1 + K_s C_e^{\frac{1}{n}}} \tag{9}$$

$$q_e = \frac{K_R C_e}{1 + \alpha_R C_e^{g}} \tag{10}$$

where C_e (mgL^{-1}) is the amount of nitrate adsorbed at equilibrium (mgg^{-1}), q_m is the maximum adsorption capacity of AC-2 (mgg^{-1}), b is Langmuir constant (Lmg^{-1}); K_f (mgg^{-1})(Lmg^{-1})$^{1/n}$ and n (gL^{-1}) are the Freundlich equilibrium constant and exponent, respectively; K_s in Sips model is the affinity of constant for adsorption (Lmg^{-1}); K_R, is the Redlich-Peterson adsorption capacity constant (Lg^{-1}), α_R and g are the Redlich-Peterson isotherm constant (Lmg^{-1}) and the exponent, respectively.

2.4.5 Thermodynamic studies

The effect of temperature on the adsorption capacity of AC-2 towards nitrate was studied at three separate temperatures such as room temperature 25°C, 35 °C and 45°C. Thermodynamic parameters were calculated using the following equations:

$$\Delta G^{\circ} = -RT\ln K \tag{11}$$

$$\Delta G^{\circ} = \Delta H^{\circ} - T\Delta S^{\circ} \tag{12}$$

substituting Eq. 11 into Eq. 12 gives:

$$lnK = -\frac{\Delta H^{\circ}}{RT} + \frac{\Delta S^{\circ}}{R} \quad (13)$$

where $\Delta G^{\circ}$is standard Gibbs free energy change (kJmol^{-1}), R is the universal gas constant (8.314 JK^{-1}mol^{-1}), T is the absolute temperature (in Kelvin), $\Delta H^{\circ}$is standard enthalpy (kJmol^{-1}), $\Delta S^{\circ}$is standard entropy (JK^{-1}mol^{-1}), and K is the unitless equilibrium constant (Eq. (14)) [33] [34].

$$K = 1000\frac{q_e}{C_e} \quad (14)$$

2.4.6 Effect of co-existing (competing) anions

The presence of co-existing anions (e.g. phosphate, carbonate, sulfate and chloride), which are commonly present in the matrix of ground water at various concentrations, might affect nitrate adsorption capacity. Therefore, a series of experiments were conducted to evaluate the influence of these competing anions by adding different concentrations of co-existing anions (20, 40, 80 and 160 mgL^{-1}) in nitrate solution (fixed nitrate concentration of 40 mgL^{-1}) for 120 min at room temperature at optimum pH and adsorbent dosage of 7 and 4 gL^{-1}, respectively. At the end of experiments, the adsorbent was separated from the solution and the residual nitrate concentration was analyzed by the aforementioned spectroscopic method.

2.5 Error analysis

The goodness of fit of the applied isotherm and kinetic models to the experimental data was evaluated using two error functions as follows:

1. The coefficient of determination (R^2)

$$R^2 = \frac{(\sum_{i=1}^{n}(O_i - O_{ave}).(P_i - P_{ave}))^2}{\sum_{i=1}^{n}(O_i - O_{ave})^2.\sum_{i=1}^{n}(P_i - P_{ave})^2} \quad (15)$$

2. The average relative error (ARE) [35]

$$ARE = \left(\frac{100}{n}\sum_{i=1}^{n} abs(\frac{O_i - P_i}{O_i})\right) \quad (16)$$

where O_{ave}, P_{ave}, n, Oi, P_i are observed average value, predicted average value, number of observations, ith of the observed and predicted value, respectively.

2.6 Column test

To evaluate the feasibility of adsorbents in continuous mode, 10 g of each adsorbent was added into a glass column (10 mm internal diameter and 200 mm length) with a bed volume of 19 cm^3. The flow rate was fixed at the same amount of 2 mL per min in the case of gravity usage. The initial concentration of nitrate was 10 mg/L. After regular intervals, effluent samples were collected for the determination of nitrate concentration. The samples were also analyzed in the terms of cationic surfactant desorption from the AC-2 surface. A spectrophotometer (DR5000 HACH) equipped with a thermal reactor was used to determine CTAB concentration. All the experiments were carried out at room temperature (25 °C) and initial pH of 7 to simulate a groundwater environment. The column experiments were pursued until the concentration of effluent was equal to the influent.

3 Results and discussion

3.1 Surface characteristics of the ACs

Fig. 1 represents FTIR spectra of the ACs. The band at wavenumber of 3418 cm^{-1} for AC (3444 for AC-1 and 3450 for AC-2) is due to OH stretching (surface hydroxyl groups and physisorbed water after chemical treatment) [36]. There was one prominent peak at 2914 cm^{-1} in the AC-2 sample spectrum which can be attributed to symmetric and asymmetric CH_2-strectching vibration associated with the cationic surfactant attached on AC-2 [21]. The band at

1575 cm^{-1} for AC (1552 for AC-1 and 1577 for AC-2) is associated with the C=C stretching of aromatic rings whose intensity is enhanced by the presence of oxygen atoms as phenol or ether groups [37]. The bands 1300-1000 cm^{-1} (1136 cm^{-1} for AC, 1154 for AC-1 and 1161 for AC-2) are assigned to C-O stretching [37]. The bands at 578 cm^{-1} for AC (532 for AC-1 and 564 for AC-2) can be ascribed to the presence of C–X vibration [38].

FTIR studies showed that the alkaline treatment did not significantly change the peaks' positions of the untreated AC compared to treated ACs. This trend has also been reported by other authors [37].

Fig. 1

Fig. 2 shows N_2 adsorption-desorption isotherms and the pore size distributions. The structural parameters of adsorbents are summarized in Table 1. According to the IUPAC (International Union of Pure and Applied Chemistry), the isotherms in this work were classified into type IV, H4.

Table 1

From Fig. 2, it can be seen that due to the existence of microporous structure, pore filling occurs at low relative pressure. The presence of adsorption hysteresis loop indicates the presence of mesoporosity according to type IV, and the porous carbon includes slit-shaped pores according to H4.

Fig. 2

In addition, these results interestingly suggested that treatment of the ACs does not have a significant impact on the pore size distribution. In this work, all the samples had similar pore size distributions, with most of the pores ranging around 2.20 nm.

The morphology of the ACs is shown in Fig. 3. All these micrographs support the N_2 adsorption analysis results. From Fig. 3b, it is clear that the alkaline treatment results in devolving more microspore structures into activated carbon. It may be attributed to the dissolution some components of the coconut shell structure by alkali; hence, the surface of the AC-1 became cleaned compared to the AC. The increase in microporosity may be helpful for increasing nitrate adsorption based on three different reasons: 1) higher surface area and micropore volume resulting in accommodating more cationic surfactant; thus, potentially availing more ion exchange sites [39]. 2) microporosity could play an important role to adsorb nitrate [14]. 3) NaOH could make most organic components soluble into water by weakening the van der Waals forces between adsorbate and micropore surface [40], hence these couldn’t pass to the solution and interfere with nitrate adsorption.

The results of SEM analysis are consistent with the results obtained from analyzing the activated carbons using N_2 adsorption isotherm. As shown in Table 1, the micropore volume increased from 0.376 (in AC) to 0.400 cm^3g^{-1} (in AC-2). These results are consistent with BET surface area where lower surface area was observed for AC (888 m^2g^{-1}) compared to AC-1 is 901 m^2g^{-1}. However, the cationic surfactant modification leads the surface area to become smooth (Fig. 3(c)); as a result, the surface area and pore volume of the activated carbon decrease. In this case, some of the micropores were completely filled with CTAB, resulting in having the lowest micropore volume among other adsorbents with 0.310 cm^3g^{-1}.

Fig. 3

3.2 Batch adsorption studies

3.2.1 Effectiveness of the commercially AC and post-treated ACs in the removal of nitrate

Fig. 4 shows nitrate removal percentage at equilibrium time for the commercially AC and post-treated ACs. As can be seen from Fig. 4, AC and AC-1 exhibited a poor performance for NO_3^- adsorption. AC-1, In spite of having higher surface area and micropore volume as compared to AC, it showed almost the same amount of adsorption. The AC-2 performance was the best among others despite having the lowest surface area and micropore volume. This behavior might be attributed to the main mechanism of nitrate adsorption. The type and amount of the functional groups on the surface of AC play a key role in adsorption of nitrate. In this case, the quaternary ammonium functional groups, left after cationic surfactant modification on the surface of AC-2, led to increase the affinity towards the nitrate. These results indicated that higher specific surface area is not necessarily guaranteed a higher adsorption capacity towards nitrate anion. In this study, AC-2 exhibited the lowest value of specific surface area among other adsorbents, in spite of its highest amount of nitrate uptake. These results were consistent with results of other researchers [5,13,14,17]. Due to the better removal efficiency evidenced for AC-2, the subsequent batch experiments were carried out by using AC-2.

Fig. 4

The combination effects of two different treatments on the surface of AC and possible mechanism of nitrate adsorption on the AC-2's surface could be further discussed as follows: cationic surfactant molecules attract into microporosity structure of AC-1 through high electrostatic attraction between the negatively charged surface of AC-1 and positive charge of cationic surfactant. The surface negative charge of AC-1 is due to ionization of abundant surface oxygen-containing functional groups at pH 7. At the CTAB concentration lower than CMC, the surfactant forms a monolayer or 'hemimicelle' at the solid-aqueous interface via strong Coulombic (ionic) bonds [41]. Nitrate is adsorbed on the positively charged segments of the surfactant attached to the AC-2 [42].

3.2.2 Effect of pH

The effect of initial pH on nitrate removal is shown in Fig. 5. When the pH changes, the amount of nitrate adsorbed on AC-2 does not significantly change. The highest nitrate adsorption occurred at pH 5 (almost the same value compared to pH 7). However, the lower pH value did not favor the higher adsorption of nitrate. As the pH of system decreases, the number of positive charged sites on AC-2 increases, thus nitrate anions adsorb on the surface of AC-2 due to electrostatic attraction. Besides, the sharp decrease of nitrate adsorption below pH 5 may be related to the competition of Cl^- ions (from adding HCl to adjust the pH) with nitrate anions. At higher pH value, the reason for a poor nitrate adsorption is that the negative charged sites on the AC-2 is increased. As a result, nitrate adsorption did not favor due to electrostatic repulsion. Similar results were also reported by other researchers [14,19,21,43,44]. Overall, the adsorption of nitrate by AC-2 is independent from pH of solution; hence, further experiments were carried out at natural pH (pH 7).

Fig. 5

3.2.3 Effect of adsorbent dosage

Adsorption of 40 mgL^{-1} nitrate with different AC-2 dosages (0.05–0.5 gL^{-1}) was carried out to evaluate its removal efficiency towards nitrate, which is shown in Fig. 6. The results showed that as the adsorbent dosage increases from 0.05 to 0.5 gL^{-1}, the nitrate percentage removal increases from 25 to 83%, whereas the adsorption capacity decreases from 11 to 3.3 mgg^{-1}. This might be due to the fact that the increased percentage removal of nitrate with increasing AC-2 dose provided the availability of more active surfaces sites of the adsorbent for adsorption. However, the decreased adsorption capacity might be attributed to the decreased total surface area of the adsorbent caused by the increase in adsorbent dose at constant nitrate concentration and volume [45]. The results also clearly indicate that beyond the AC-2 dosage of 4 gL^{-1}, the percent removal increases slowly, which indicates that 4 gL^{-1} is the optimum adsorbent dosage.

Fig. 6

3.2.4 Effect of contact time

Fig. 7 shows the effect of contact time on nitrate adsorption with two different initial nitrate concentrations of 40 and 80 mgL^{-1} at an optimum adsorbent dosage and optimum pH. The availability of plenty actives sites on the AC-2's surface led to a rapid uptake of nitrate in the beginning. As can be seen in Fig. 7, the time required for equilibrium adsorption is 120 min. With further increasing time, the diminishing availability of the remaining active sites and the decrease in the driving force make it take long time to reach equilibrium. Thus, the adsorption rate becomes slower. Equilibrium time does not change with increasing initial nitrate concentration from 40 to 80 mgL^{-1}, while the amount of nitrate adsorbed is increased with increase in initial nitrate concentration. The contact time of 120 min was selected as the equilibrium time for further experiments.

Fig. 7

3.2.5 Adsorption kinetics

Understanding the reaction pathway and mechanism of the adsorption process are achieved through a study of adsorption kinetics [46,47]. In this study, To investigate the mechanism of adsorption and potential rate controlling steps such as chemical reaction, diffusion control, and mass transport processes, three kinetic models, namely pseudo-first-order, pseudo-second-order, and intra-particle diffusion models were used to test the experimental data to determine which one can best describe the adsorption reactions. The pseudo-first-order model is on the following assumption: the sorption rate abates linearly with the adsorption capacity [47]. The pseudo-second-order kinetic model is usually utilized to elucidate a chemical sorption and it considers the rate-limiting step is the interaction between two reagent particles [48]. The intra-particle diffusion kinetic model is used to prove that the mechanism of adsorption is controlled by diffusion, where the rate of adsorption process is dependent upon the diffusion speed of adsorbate through adsorbent [28]. The obtained values of the used kinetic models are listed in Table 2 and the fitted models to the experimental data are represented in Fig 8a. All the experimental data showed better compliance with the pseudo-second-order kinetic model in the terms of high correlation coefficients (R^2) and lower values of ARE at both initial concentration of 40 and 80 mgL^{-1}. Furthermore, the similarity between the experimental q_e values and q_e values calculated from the model indicate that the adsorption of nitrate onto AC-2 fits better to the pseudo-second-order model as compared to the other models for adsorption of nitrate (Table 2). Such a finding is also in good agreement with previous studies [4,13,14,24,43,47]. Moreover, the rate constant (k_2) of the pseudo-second-order equation decreases with increasing initial nitrate concentration, demonstrating that nitrate adsorption may be more favorable at low solute concentration.

The possibility of intra-particle diffusion resistance affecting adsorption was explored by using the intra-particle diffusion model. A plot of q_t vs. $t^{1/2}$ is shown in Fig. 8b. This curve comprised three distinct sections: initial curved or steep-sloped portion represents the bulk diffusion or exterior adsorption rate which is very high, the subsequent linear portion is attributed to the intra-particle diffusion, and plateau portion represents the equilibrium [49]. The k_{id}, θ and correlation coefficient were calculated from this plot. As can be seen from this Fig. 8b, and Table 2 the intercept of the line, do not pass through the origin at two concentrations studied indicating that the mechanism of nitrate adsorption onto adsorbent does not follow this model, similar to former reports [47,50,51].

Fig.8

Table 2

3.2.6 Adsorption isotherms

Adsorption isotherms are the fundamental requirements for correlation of the adsorbate concentration in an aqueous phase with its concentration in adsorbate/adsorbent interface. It is of importance to achieve the most appropriate correlation for the equilibrium curves to optimize the design of the adsorption systems [52]. Various isotherm models such as Langmuir, Freundlich, Sips and Redlich-Peterson were used to evaluate the equilibrium characteristics of adsorption processes. The Langmuir isotherm model assumes monolayer coverage on a homogeneous surface without interaction between adsorbed molecules and uniform energies of adsorption onto the surface [13]. The maximum adsorption capacity of adsorbent regarding monolayer adsorption on the surface of adsorbent can be estimated via using the Langmuir model [53]. On the other hand, the Freundlich equation is an empirical equation based on adsorption on a heterogeneous surface and is not restricted to the formation of the monolayer [54]. The Sips and Redlich-Peterson adsorption isotherm models combine the features of Langmuir and Freundlich isotherms. They approach the Langmuir and Freundlich isotherms at low and high adsorbate concentration, respectively [47,53,55].

The corresponding parameters, correlation coefficients and values of ARET are listed in Table 3 and the results of Langmuir, Freundlich, Sips and Redlich-Peterson fitting are shown in Fig. 9. Applicability of the isotherm models to describe the adsorption process was judged by the correlation coefficient (R^2) values and values of average relative error (ARE). Table 3 shows that the Langmuir isotherm has the higher correlation coefficient (0.99) and lower value of ARE (5.44), indicating that this model fits the experimental data well. Several researchers have also reported that the Langmuir model was more appropriate for describing the adsorption isotherm of nitrate onto ACs and treated ACs [14,47,51].

Fig. 9

Table 3

The essential characteristics of Langmuir isotherm can be expressed in terms of a dimensionless equilibrium parameter (R_L) which is defined as the following equation [37,56]:

$$R_L = \frac{1}{1+bC_0} \tag{17}$$

where C_0 is the initial nitrate concentration (mgL^{-1}). The adsorption is considered as irreversible when $R_L = 0$, favorable when $0 < R_L < 1$, linear when $R_L = 1$, and unfavorable when $R_L > 1$. As can be observed in Table 3, the range of R_L values at initial concentration of 40–200 mg/L nitrate was 0.08–0.29 confirming that the adsorption isotherm is favorable. The n value in Freundlich model indicates the type of isotherm. The obtained value of n (Table 3) is 2.94 $(1 < n < 10)$ indicating that nitrate is favorably adsorbed onto the AC-2 under the studied conditions.

Table 4 presents a comparison of the maximum nitrate adsorption capacity of AC-2 (this work) with other ACs, as evaluated according to the Langmuir model. As can be observed, AC-2 with maximum adsorption capacity of 21.51 mgg^{-1} has similar or even higher adsorption capacity compared with ACs and treated ACs, reported by other researchers.

Table 4

3.2.7 Thermodynamic parameters

To evaluate the feasibility and nature of the adsorption reaction, the thermodynamic parameters such as standard Gibbs free energy change (ΔG°), standard enthalpy (ΔH°) and standard entropy (ΔS°) were determined. The slope and intercept of the fitted straight line to the plot ΔG°versus T (R^2=0.98) gives the values of $\Delta H^{\circ}$and ΔS°, respectively (figure not shown). The corresponding thermodynamic parameters are tabulated in Table 5. The value of enthalpy change $\Delta H^{\circ}$is negative indicating adsorption is exothermic in nature. Other researchers have also documented that nitrate adsorption is exothermic [14,21]. The negative values obtained for ΔG° at all three temperatures confirm the feasibility of the process and spontaneous nature of the adsorption process. Since the obtained values of $\Delta G^{\circ}$are lower than -10 kJmol^{-1}, it can be indicative of occurrence of physical adsorption during the adsorption process [47]. The negative value of ΔS°corresponds to a decrease in the degree of freedom of the adsorbed species, which is in consistent with the previous study [14].

Table 5

3.2.8 Effect of co-existing (competing) anions

In the present study, all experiments were carried out in the batch mode with the single anion, i.e. nitrate. However, in the real system, several other anions are present which can compete with nitrate. Therefore, the effect of competing anions including phosphate, carbonate, sulfate and chloride was examined on the adsorption of nitrate by AC-2 in a solution containing varying concentration of competing anions (20, 40, 80 and 160 mgL^{-1}) and a fixed nitrate concentration of 40 mgL^{-1}. The experiment was conducted at the optimum conditions (e.g. pH 7, 25°C, 4 gL^{-1} as adsorbent dosage and contact time of 120 min). The results are presented in Fig. 10. The reduction in adsorption capacity of nitrate was found to be highest for sulfate, followed by chloride and phosphate, while there was no sign of significant change in the presence of carbonate. The result shows that the inhibition effect was insignificant for carbonate and phosphate, mainly due to the formation of other species (e.g. H_2CO_3 and $H2PO_4^-$) with lower tendency to compete with nitrate for adsorption site of AC-2 in the pH of 7 during the experiment. These results are consistent with the results obtained by other researchers [21].

Fig. 10

3.3 Column test

The feasibility of each adsorbent to treat synthetic nitrate solution was investigated in small column experiments. Fig. 11 presents the breakthrough curve of each adsorbent. As can be observed, each step of modifications leads to increase the lifetime of adsorbents. In the case of AC-2, the breakthrough was 54 bed volume (BV), while BV was 6.8 and ∼0 for AC-1 and AC, respectively. This improvement in the lifetime indicates the feasibility of using AC-2 in continuous condition to remove nitrate from aqueous solution compared to the other adsorbents. Release of the cationic surfactant from the surface of AC-2 was also investigated during the column test. Presence of cationic surfactants into water can create health hazards due to toxic nature [23,57]. For this reason, the amount of surfactants was analyzed in the effluent of the column. Within the lifetime of AC-2, the surfactant was not detected.

Fig. 11

4 Conclusions

Present study exhibits the use of two different steps of treatments on commercial AC to enhance nitrate uptake from aqueous solution. Combination of alkaline treatment followed by cationic surfactant treatment led to increase the nitrate adsorption effectively. It was found that this effectiveness was mainly due to a significant increment in the number of functional groups after cationic surfactant treatment, while surface area and porous structure of AC did not seem to play a key role in the nitrate uptake. The results also demonstrated that alkaline treatment could be used before the cationic surfactant treatment to improve the performance of AC without adverse effect on its physicochemical properties. AC-2 adsorption capacity towards nitrate was found to be independent at different pH values. The optimum adsorbent dosage and equilibrium time were found to be $4gL^{-1}$ and 120 min, respectively. The maximum nitrate adsorption capacity, as evaluated according to the Langmuir model, was found to be 21.51 mgg^{-1}. The adsorption was well described by pseudo-second-order kinetic model. In column experiments, the breakthrough point of AC-2 was 54 bed volumes (BV), while that of untreated AC and alkaline treated AC were 6.8 and ~ 0 BV, respectively. In the effluent of column, the release of surfactant from AC-2's surface was not observed during the lifetime of AC-2. All these advantages recommend that the AC-2 could be used as a promising adsorbent in order to remove nitrate from water.

List of symbols:

q_e: Adsorption capacity at equilibrium time (mgg^{-1})

$(q_e)_{Cal.}$: Calculated adsorption capacity at equilibrium (mgg^{-1})

$(q_e)_{Exp.}$: Experimental adsorption capacity at equilibrium (mgg^{-1})

q_t: Adsorption capacity (mgg^{-1}) at time t (min)

C_0: Initial nitrate concentration (mgL^{-1})

C_e: Equilibrium nitrate concentration (mgL^{-1})

V: Volume of the solution (L)

m: Mass of the adsorbent (g)

k_1: Lagergren's rate constant of adsorption (min^{-1})

k_2: Rate constant of pseudo-second-order (gmg^{-1} min^{-1})

k_{id}: Intra-particle diffusion rate constant (mgg^{-1}min$^{-1/2}$)

θ: Constant related to the thickness of the boundary layer (mgg^{-1})

q_m: Maximum adsorption capacity reflected a complete monolayer (mgg^{-1})

b: Langmuir constant (Lmg^{-1})

K_F: Adsorption capacity at unit concentration (mgg^{-1})(Lmg^{-1})$^{1/n}$

n: Adsorption intensity of Freundlich model (gL^{-1})

K_s: Sips isotherm model constant (Lmg^{-1})

$K_{R:}$ Redlich–Peterson isotherm constant (Lg^{-1})

$\alpha_{R:}$ Redlich–Peterson isotherm constant (Lmg^{-1})

g: Redlich–Peterson isotherm exponent

T: Absolute temperature (K)

R: Universal gas constant (8.314 J mol^{-1} K^{-1})

ΔG°: Standard Gibbs free energy change (kJmol^{-1})

ΔH°: Standard enthalpy (kJmol^{-1})

ΔS°: Standard entropy (Jmol^{-1}K^{-1})

K: Unitless equilibrium constant

O_{ave}: observed average value

P_{ave}: predicted average value

5 References

[1] J. Pacheco, A. Cabrera, Groundwater contamination by nitrates in the Yucatan Peninsula, Mexico, Hydrogeol. J. 5 (1997) 47–53.

[2] R.F. Spalding, M.E. Exner, Occurrence of nitrate in groundwater—a review, J. Environ. Qual. 22 (1993) 392–402.

[3] A. Kapoor, T. Viraraghavan, Nitrate removal from drinking water-review, J. Environ. Eng. 123 (1997) 371–380.

[4] T. Iida, Y. Amano, M. Machida, F. Imazeki, Effect of surface property of activated carbon on adsorption of nitrate ion, Chem. Pharm. Bull. 61 (2013) 1173–1177.

[5] K. Ota, Y. Amano, M. Aikawa, M. Machida, Removal of nitrate ions from water by activated carbons (ACs)—Influence of surface chemistry of ACs and coexisting chloride and sulfate ions, Appl. Surf. Sci. 276 (2013) 838–842.

[6] S. Chen, W. Wu, K. Hu, W. Li, The effects of land use change and irrigation water resource on nitrate contamination in shallow groundwater at county scale, Ecol. Complex. 7 (2010) 131–138.

[7] P. Rao, K. Puttanna, Nitrates, agriculture and environment, Curr. Sci. 79 (2000) 1163–1169.

[8] F.T. Wakida, D.N. Lerner, Non-agricultural sources of groundwater nitrate: a review and case study, Water Res. 39 (2005) 3–16.

[9] L. Fewtrell, Drinking-water nitrate, methemoglobinemia, and global burden of disease: a discussion, Environ. Health Perspect. (2004) 1371–1374.

[10] A. Esmaeili, F. Moore, B. Keshavarzi, Nitrate contamination in irrigation groundwater, Isfahan, Iran, Environ. Earth Sci. 72 (2014) 2511–2522.

[11] WHO, Guidelines for drinking-water quality 4th edition, World Heal. Organ. (2011).

[12] EPA, Drinking Water Standards and Health Advisories Tables, US Environ. Prot. Agency. (2012).

[13] M.A. Tofighy, T. Mohammadi, Nitrate removal from water using functionalized carbon nanotube sheets, Chem. Eng. Res. Des. 90 (2012) 1815–1822.

[14] A. Bhatnagar, M. Ji, Y. Choi, W. Jung, S. Lee, S.S. Kim, G. Lee, H. Suk, H. Kim, B. Min, S.S. Kim, B. Jeon, J. Kang, Removal of Nitrate from Water by Adsorption onto Zinc Chloride Treated Activated Carbon, Sep. Sci. Technol. 43 (2008) 886–907.

doi:10.1080/01496390701787461.

[15] G. V Nunell, M.E. Fernández, P.R. Bonelli, A.L. Cukierman, Conversion of biomass from an invasive species into activated carbons for removal of nitrate from wastewater, Biomass and Bioenergy. 44 (2012) 87–95.

[16] A.S. Adeleye, J.R. Conway, K. Garner, Y. Huang, Y. Su, A.A. Keller, Engineered nanomaterials for water treatment and remediation: Costs, benefits, and applicability, Chem. Eng. J. 286 (2016) 640–662. doi:http://dx.doi.org/10.1016/j.cej.2015.10.105.

[17] G. V Nunell, M.E. Fernandez, P.R. Bonelli, A.L. Cukierman, Nitrate uptake improvement by modified activated carbons developed from two species of pine cones, J. Colloid Interface Sci. 440 (2015) 102–108.

[18] A. Bhatnagar, M. Sillanpää, A review of emerging adsorbents for nitrate removal from water, Chem. Eng. J. 168 (2011) 493–504. doi:http://dx.doi.org/10.1016/j.cej.2011.01.103.

[19] A. Afkhami, T. Madrakian, Z. Karimi, The effect of acid treatment of carbon cloth on the adsorption of nitrite and nitrate ions, J. Hazard. Mater. 144 (2007) 427–431.

[20] A. Rezaee, H. Godini, S. Dehestani, A. Khavanin, Application of impregnated almond shell activated carbon by zinc and zinc sulfate for nitrate removal from water, Iranian J. Environ. Health Sci. Eng. 5 (2008) 125–130.

[21] D.-W. Cho, C.-M. Chon, Y. Kim, B.-H. Jeon, F.W. Schwartz, E.-S. Lee, H. Song, Adsorption of nitrate and Cr (VI) by cationic polymer-modified granular activated carbon, Chem. Eng. J. 175 (2011) 298–305.

[22] S. Wang, Z.H. Zhu, A. Coomes, F. Haghseresht, G.Q. Lu, The physical and surface chemical characteristics of activated carbons and the adsorption of methylene blue from wastewater, J. Colloid Interface Sci. 284 (2005) 440–446. doi:http://dx.doi.org/10.1016/j.jcis.2004.10.050.

[23] C.A. Basar, A. Karagunduz, A. Cakici, B. Keskinler, Removal of surfactants by powdered activated carbon and microfiltration, Water Res. 38 (2004) 2117–2124.

[24] H.-D. Choi, W.-S. Jung, J.-M. Cho, B.-G. Ryu, J.-S. Yang, K. Baek, Adsorption of Cr (VI) onto cationic surfactant-modified activated carbon, J. Hazard. Mater. 166 (2009) 642–646.

[25] A. Rahmani, H.Z. Mousavi, M. Fazli, Effect of nanostructure alumina on adsorption of heavy metals, Desalination. 253 (2010) 94–100. doi:10.1016/j.desal.2009.11.027.

[26] S. Lagergren, About the theory of so-called adsorption of soluble substances, 24 (1898) 1–39.

[27] Y.-S. Ho, G. McKay, Pseudo-second order model for sorption processes, Process Biochem. 34 (1999) 451–465. doi:10.1016/S0032-9592(98)00112-5.

[28] W.J. Weber, J.C. Morris, Kinetics of adsorption on carbon from solution, J. Sanit. Eng. Div. 89 (1963) 31–59.

[29] I. Langmuir, The adsorption of gases on plane surfaces of glass, mica and platinum., J. Am. Chem. Soc. 40 (1918) 1361–1403.

[30] H.M.F. Freundlich, Over the adsorption in solution, J. Phys. Chem. 57 (1906) 385–471.

[31] R. Sips, Combined form of Langmuir and Freundlich equations, J. Chem. Phys. 16 (1948) 490–495.

[32] K. Vijayaraghavan, T.V.N. Padmesh, K. Palanivelu, M. Velan, Biosorption of nickel (II) ions onto Sargassum wightii: application of two-parameter and three-parameter isotherm models, J. Hazard. Mater. 133 (2006) 304–308.

[33] S. Canzano, P. Iovino, S. Salvestrini, S. Capasso, Comment on “Removal of anionic dye

Congo red from aqueous solution by raw pine and acid-treated pine cone powder as adsorbent: Equilibrium, thermodynamic, kinetics, mechanism and process design," Water Res. 46 (2012) 4314–4315.

[34] S. Dawood, T.K. Sen, Author's Responses to the comment by Canzano et al and also corrigendum to "Removal of anionic dye Congo red from aqueous solution by raw pine and acid-treated pine cone powder as adsorbent: Equilibrium, thermodynamic, kinetics, mechanism and process desi, Water Res. 46 (2012) 4316–4317.

[35] A. Kapoor, R.T. Yang, Correlation of equilibrium adsorption data of condensible vapours on porous adsorbents, Gas Sep. Purif. 3 (1989) 187–192.

[36] S.-J.J. Park, Y.-S.S. Jang, Pore structure and surface properties of chemically modified activated carbons for adsorption mechanism and rate of Cr(VI), J Colloid Interface Sci. 249 (2002) 458–463. doi:10.1006/jcis.2002.8269.

[37] B. Hayati, N.M. Mahmoodi, Modification of activated carbon by the alkaline treatment to remove the dyes from wastewater: mechanism, isotherm and kinetic, Desalin. Water Treat. 47 (2012) 322–333. doi:10.1080/19443994.2012.696429.

[38] K. Mahapatra, D.S. Ramteke, L.J. Paliwal, Production of activated carbon from sludge of food processing industry under controlled pyrolysis and its application for methylene blue removal, J. Anal. Appl. Pyrolysis. 95 (2012) 79–86.

[39] J. Patterson, R. Parette, F.S. Cannon, C. Lutes, T. Henderson, Competition of anions with perchlorate for exchange sites on cationic surfactant-tailored GAC, Environ. Eng. Sci. 28 (2011) 249–256.

[40] K. Sun, J. Jiang, J. Xu, Chemical regeneration of exhausted granular activated carbon used in citric acid fermentation solution decoloration, Iran. J. Chem. Chem. Eng. Vol. 28 (2009).

[41] J. Ma, Y.-Z. Jia, Y. Jing, J.-H. Sun, Y. Yao, X.-H. Wang, Equilibrium models and kinetic for the adsorption of methylene blue on Co-hectorites, J. Hazard. Mater. 175 (2010) 965–969.

[42] P. Loganathan, S. Vigneswaran, J. Kandasamy, Enhanced removal of nitrate from water using surface modification of adsorbents – A review, J. Environ. Manage. 131 (2013) 363–374. doi:http://dx.doi.org/10.1016/j.jenvman.2013.09.034.

[43] N. Öztürk, T.E. Bektaş, Nitrate removal from aqueous solution by adsorption onto various materials, J. Hazard. Mater. 112 (2004) 155–162.

[44] K. Ohe, Y. Nagae, S. Nakamura, Y. Baba, Removal of nitrate anion by carbonaceous materials prepared from bamboo and coconut shell, J. Chem. Eng. Japan. 36 (2003) 511–515.

[45] Y. Li, Q. Du, T. Liu, J. Sun, Y. Jiao, Y. Xia, L. Xia, Z. Wang, W. Zhang, K. Wang, Equilibrium, kinetic and thermodynamic studies on the adsorption of phenol onto graphene, Mater. Res. Bull. 47 (2012) 1898–1904.

[46] M. Doltabadi, H. Alidadi, M. Davoudi, Comparative study of cationic and anionic dye removal from aqueous solutions using sawdust-based adsorbent, Environ. Prog. Sustain. Energy. (2016).

[47] L.D. Hafshejani, A. Hooshmand, A.A. Naseri, A.S. Mohammadi, F. Abbasi, A. Bhatnagar, Removal of nitrate from aqueous solution by modified sugarcane bagasse biochar, Ecol. Eng. 95 (2016) 101–111.

[48] F. Zhang, J. Lan, Y. Yang, T. Wei, R. Tan, W. Song, Adsorption behavior and mechanism of methyl blue on zinc oxide nanoparticles, J. Nanoparticle Res. 15 (2013) 2034.

doi:10.1007/s11051-013-2034-2.

[49] N.S. Randhawa, N.N. Das, R.K. Jana, Adsorptive remediation of Cu (II) and Cd (II) contaminated water using manganese nodule leaching residue, Desalin. Water Treat. 52 (2014) 4197–4211.

[50] A. Olgun, N. Atar, S. Wang, Batch and column studies of phosphate and nitrate adsorption on waste solids containing boron impurity, Chem. Eng. J. 222 (2013) 108–119.

[51] H. Demiral, G. Gündüzoğlu, Removal of nitrate from aqueous solutions by activated carbon prepared from sugar beet bagasse, Bioresour. Technol. 101 (2010) 1675–1680. doi:10.1016/j.biortech.2009.09.087.

[52] B. Armagan, F. Toprak, Optimum isotherm parameters for reactive azo dye onto pistachio nut shells: comparison of linear and non-linear methods, Pol. J. Environ. Stud. 22 (2013) 1007.

[53] M. Baghdadi, E. Ghaffari, B. Aminzadeh, Removal of carbamazepine from municipal wastewater effluent using optimally synthesized magnetic activated carbon: Adsorption and sedimentation kinetic studies, J. Environ. Chem. Eng. 4 (2016) 3309–3321.

[54] Y. Li, P. Zhang, Q. Du, X. Peng, T. Liu, Z. Wang, Y. Xia, W. Zhang, K. Wang, H. Zhu, Adsorption of fluoride from aqueous solution by graphene, J. Colloid Interface Sci. 363 (2011) 348–354.

[55] K.Y. Foo, B.H. Hameed, Insights into the modeling of adsorption isotherm systems, Chem. Eng. J. 156 (2010) 2–10.

[56] V. Fierro, V. Torné-Fernández, D. Montané, A. Celzard, Adsorption of phenol onto activated carbons having different textural and surface properties, Microporous Mesoporous Mater. 111 (2008) 276–284.

[57] R. Mahmudov, C.P. Huang, Selective adsorption of oxyanions on activated carbon exemplified by Filtrasorb 400 (F400), Sep. Purif. Technol. 77 (2011) 294–300.

[58] P.C. Mishra, R.K. Patel, Use of agricultural waste for the removal of nitrate-nitrogen from aqueous medium, J. Environ. Manage. 90 (2009) 519–522.

Figure caption:

Fig. 1. FTIR spectra of the (a) AC, (b) AC-1, and (c) AC-2.

Fig 2. Adsorption–desorption isotherms of nitrogen at 77 K on AC, AC-1, AC-2. The insert shows the BJH pore size distribution calculated from the desorption branch of the isotherm.

Fig. 3. SEM images (a) AC, (b) AC-1, and (C) AC-2.

Fig. 4. Nitrate removal at equilibrium time for the AC, AC-1, and AC-2 (C_i=40 mg/L, temperature=25°C, adsorbent dosage=0.2 g/50 mL).

Fig. 5. Effect of initial pH on nitrate adsorption by AC-2 (C_i=40 mg/L, temperature=25°C, adsorbent dosage=0.2 g/50 mL, contact time=120 min).

Fig. 6. Effect of adsorbent dosage on nitrate removal by AC-2 (Ci=40 mg/L, temperature=25°C, pH=7, contact time=120 min).

Fig. 7. The effect of contact time on nitrate adsorption by AC-2 (temperature=25° C, adsorbent dosage=4 g/L, pH=7 at two diffirent nitrate concentration of 40 and 80 mgL^{-1}).

Fig. 8. Adsorption kinetics of nitrate adsorption by AC-2: (a) pseudo-first-order and pseudo-second-order, and (b) intra-particle diffusion models, markers are experimental data, while straight lines represent fits to the aforementioned model.

Fig. 9. Different isotherm models for nitrate adsorption by AC-2 (temperature=25° C, adsorbent dosage=0.2 g/50 mL, pH=7).

Fig. 10. Effects of presence other anions on nitrate adsorption capacity of AC-2 (temperature=25° C, adsorbent dosage=0.2 g/50 mL, pH=7, initial nitrate concentration=40 mgL^{-1}, initial co-existing anions=0-160 mgL^{-1}, contact time=120 min).

Fig. 11. Breakthrough curves of AC, AC-1, and AC-2 (initial concentration of NO_3^-=10 mg/L, temperature=25°C, flow reate= 2 mL/min, pH=7, empty bed contact time (EBCT)=9.5 min).

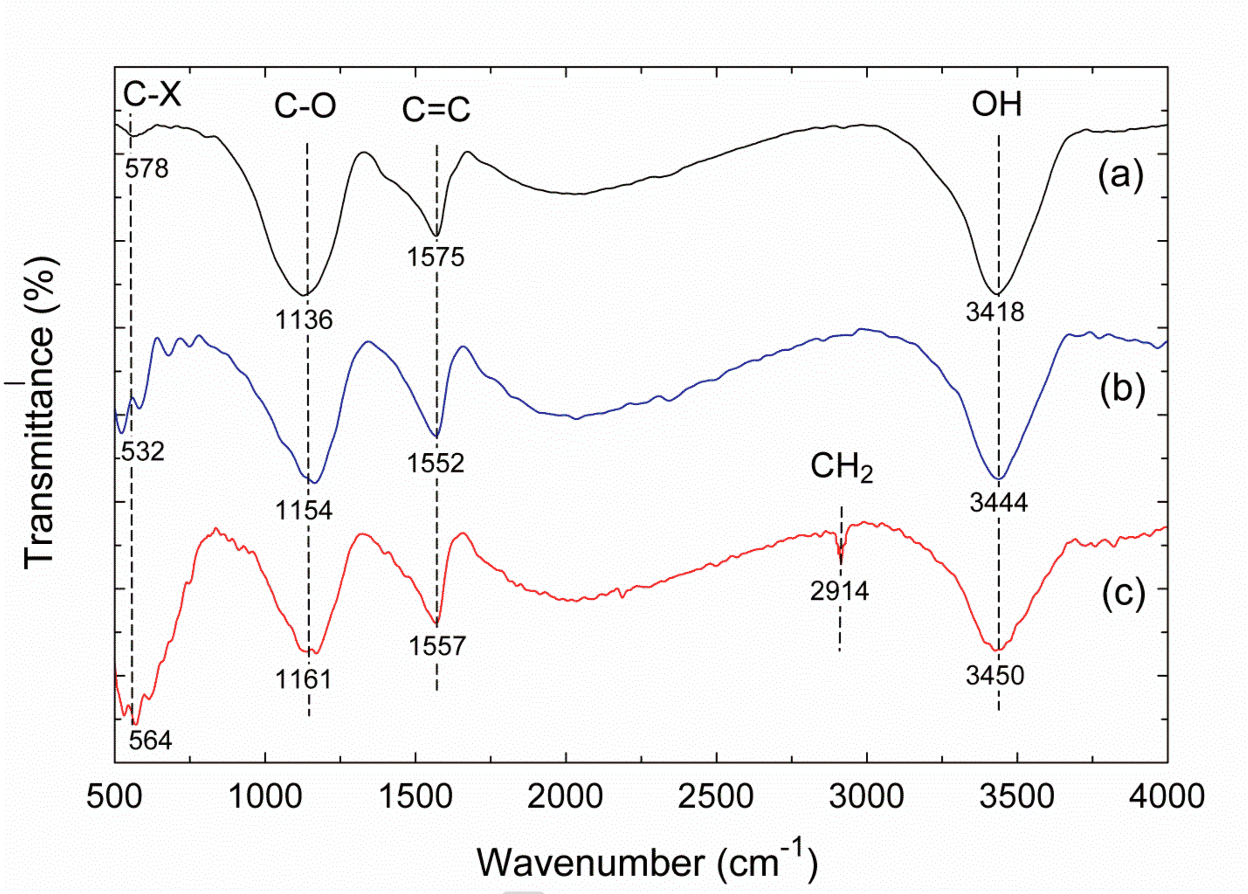

Fig. 1. FTIR spectra of the (a) AC, (b) AC-1, and (c) AC-2.

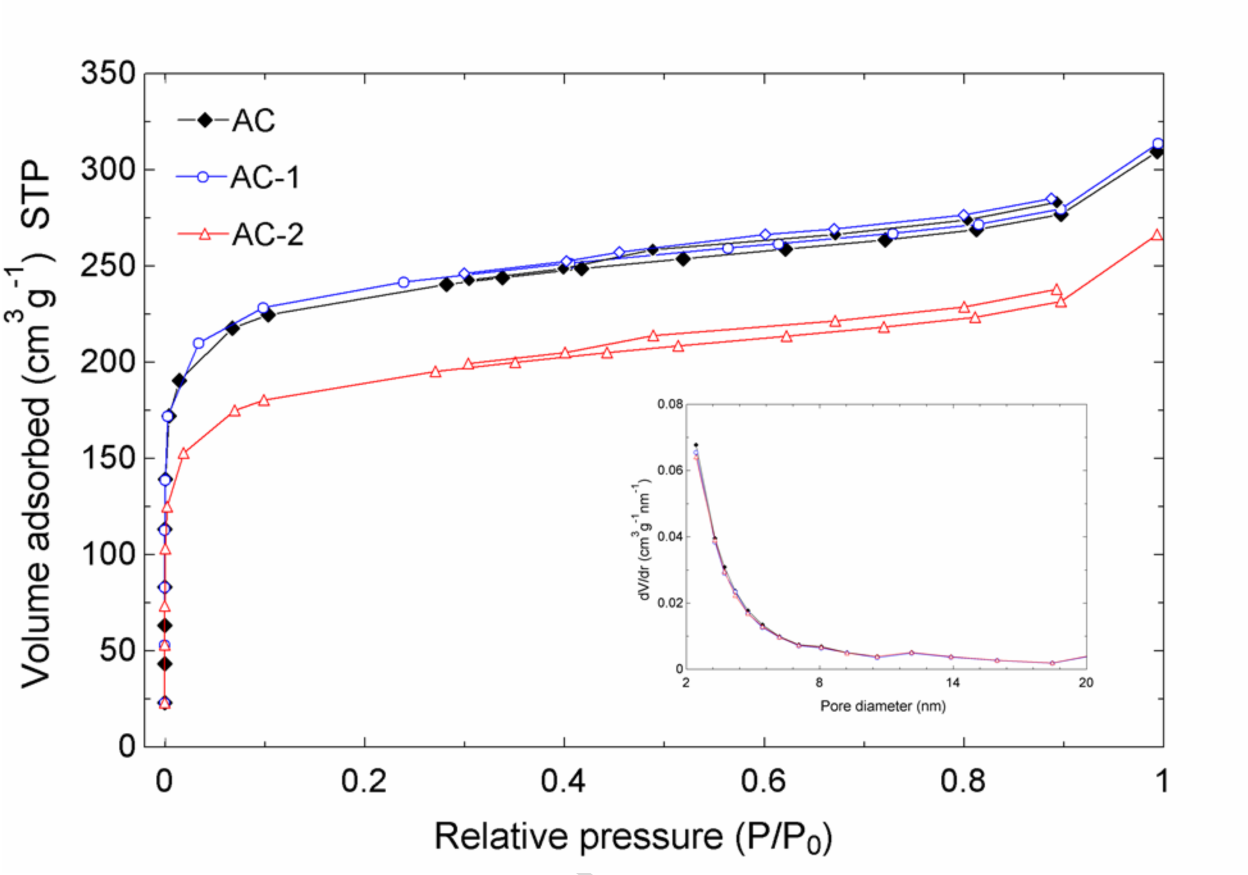

Fig. 2. Adsorption–desorption isotherms of nitrogen at 77 K on AC, AC-1, AC-2. The inset shows the BJH pore size distribution calculated from the desorption branch of the isotherm.

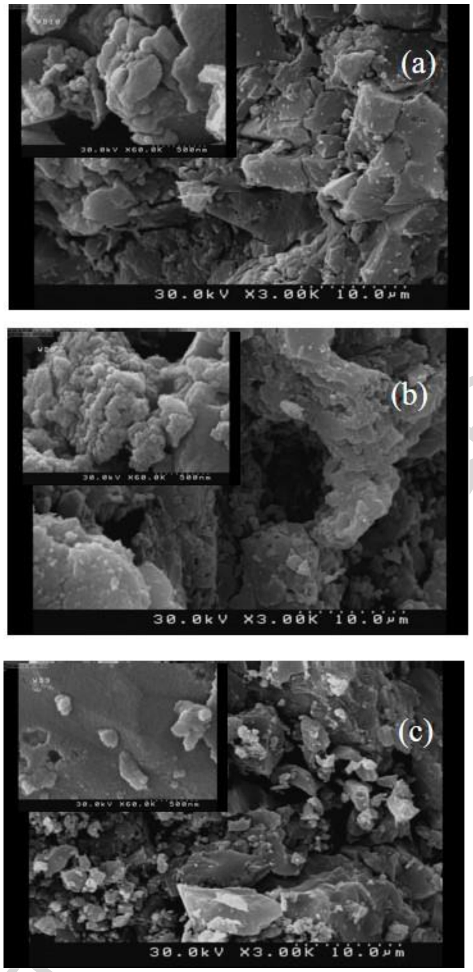

Fig. 3. SEM images (a) AC, (b) AC-1, and (C) AC-2.

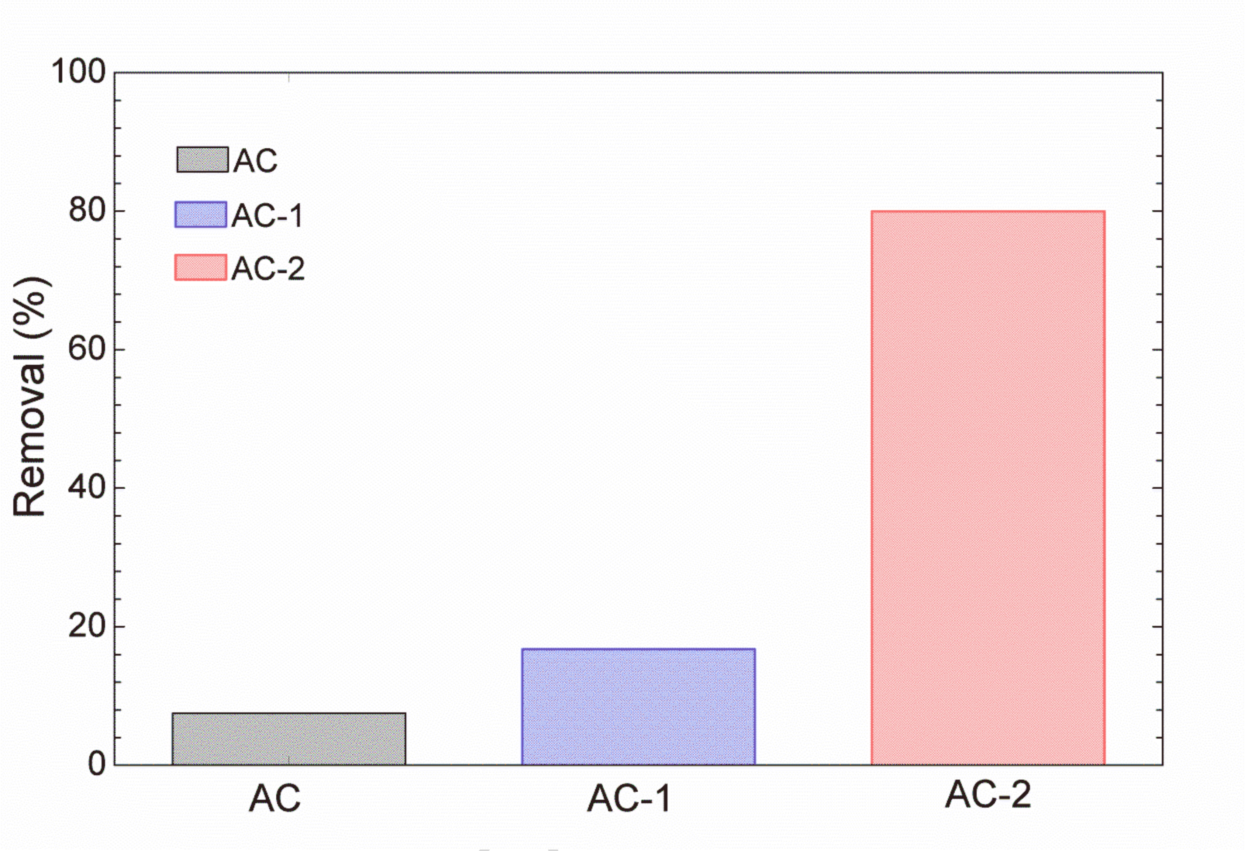

Fig. 4. Nitrate removal at equilibrium time for the AC, AC-1, and AC-2 (C_i=40 mg/L, temperature=25°C, adsorbent dosage=0.2 g/50 mL).

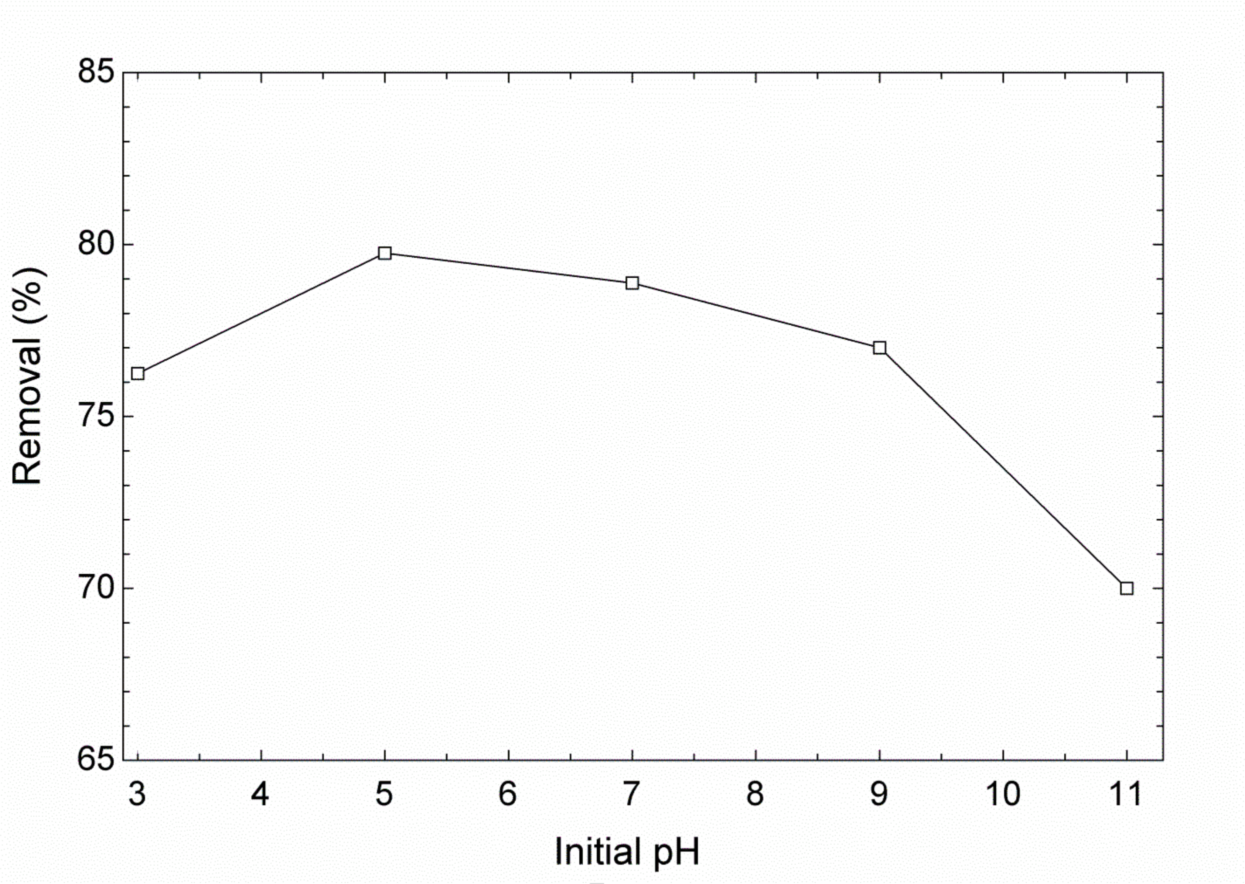

Fig. 5. Effect of initial pH on nitrate adsorption by AC-2 (C_i=40 mg/L, temperature=25°C, adsorbent dosage=0.2 g/50 mL, contact time=120 min).

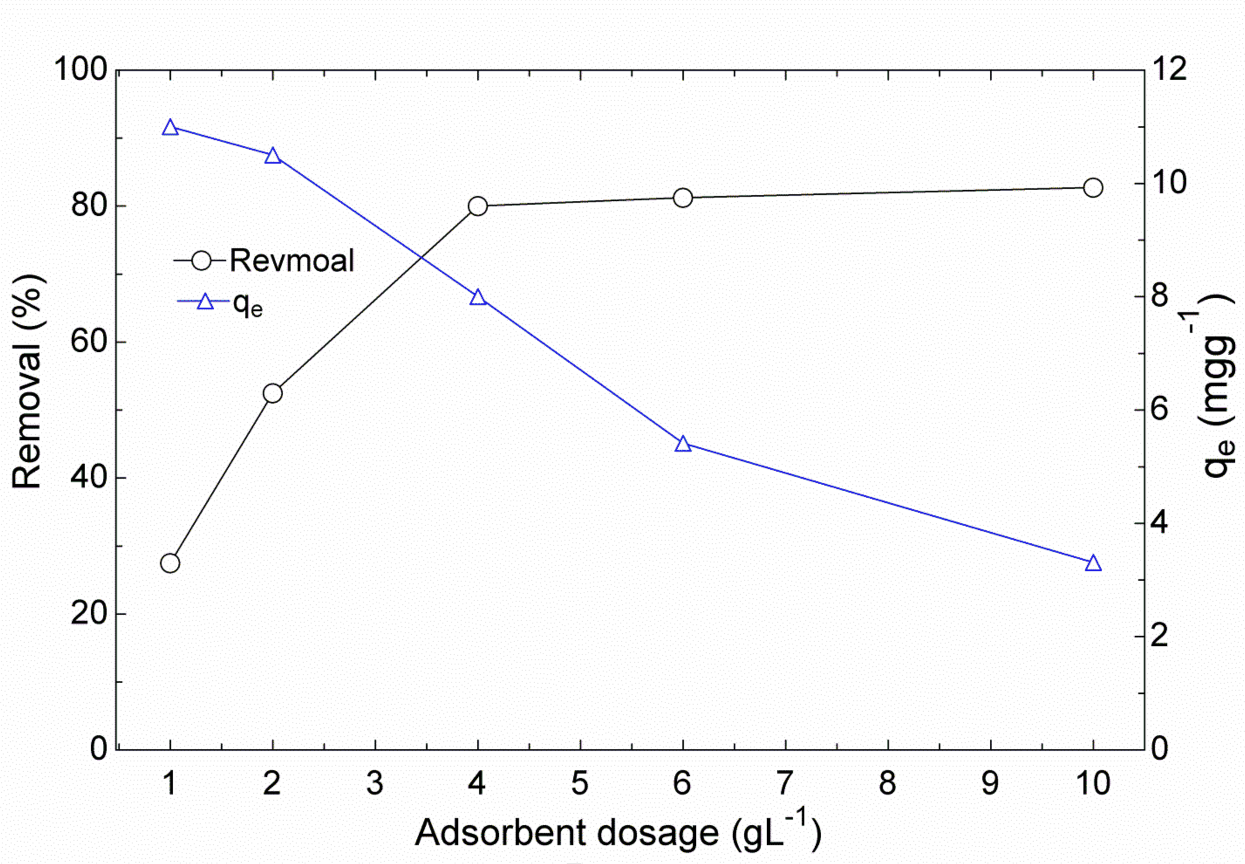

Fig. 6. Effect of adsorbent dosage on nitrate removal by AC-2 (Ci=40 mg/L, temperature=25°C, pH=7, contact time=120 min).

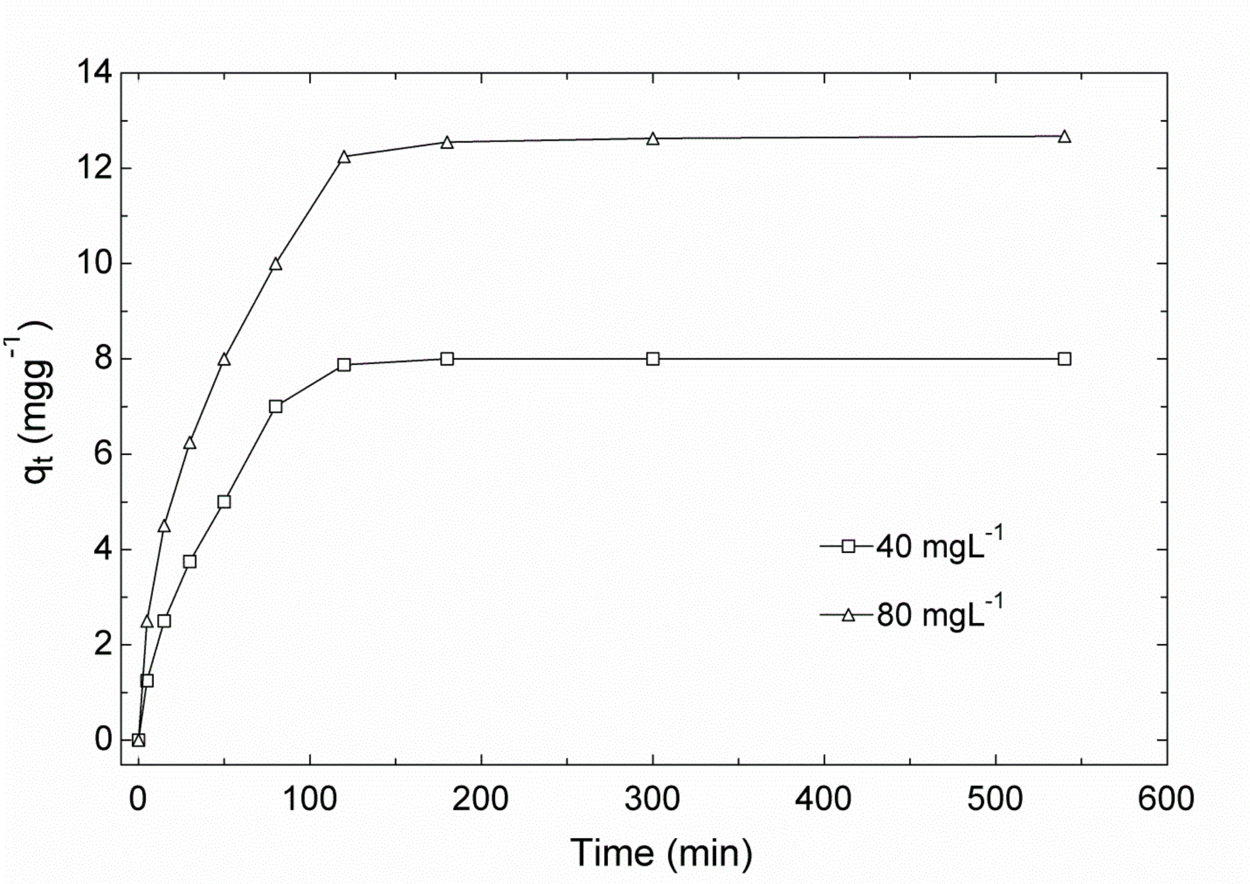

Fig. 7. The effect of contact time on nitrate adsorption by AC-2 (temperature=25° C, adsorbent dosage=4 g/L, pH=7 at two diffirent nitrate concentrations of 40 and 80 mgL^{-1}).

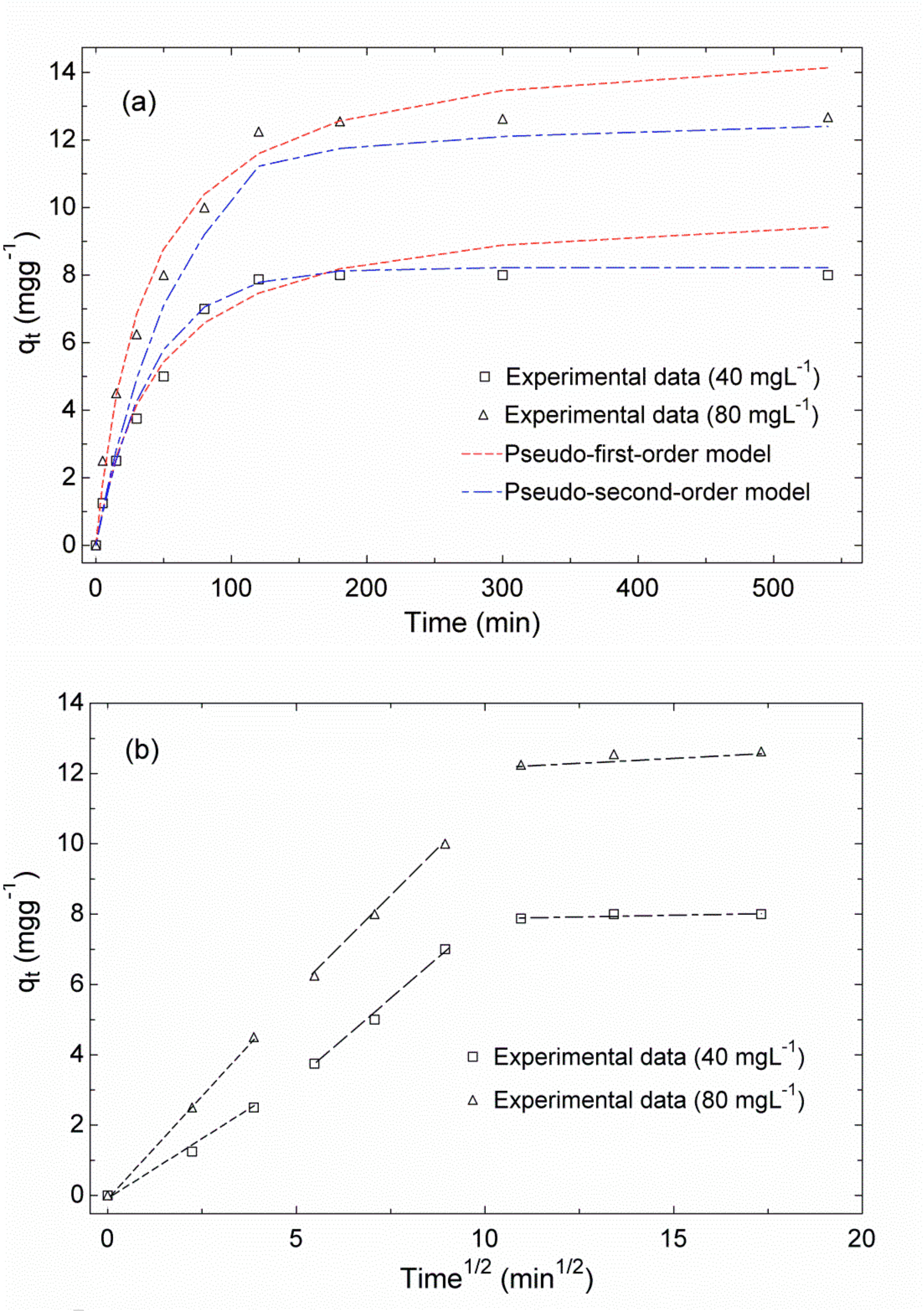

Fig. 8. Adsorption kinetics of nitrate adsorption by AC-2: (a) pseudo-first-order and pseudo-second-order, and (b) intra-particle diffusion models; markers are experimental data, while straight lines represent fits to the aforementioned model.

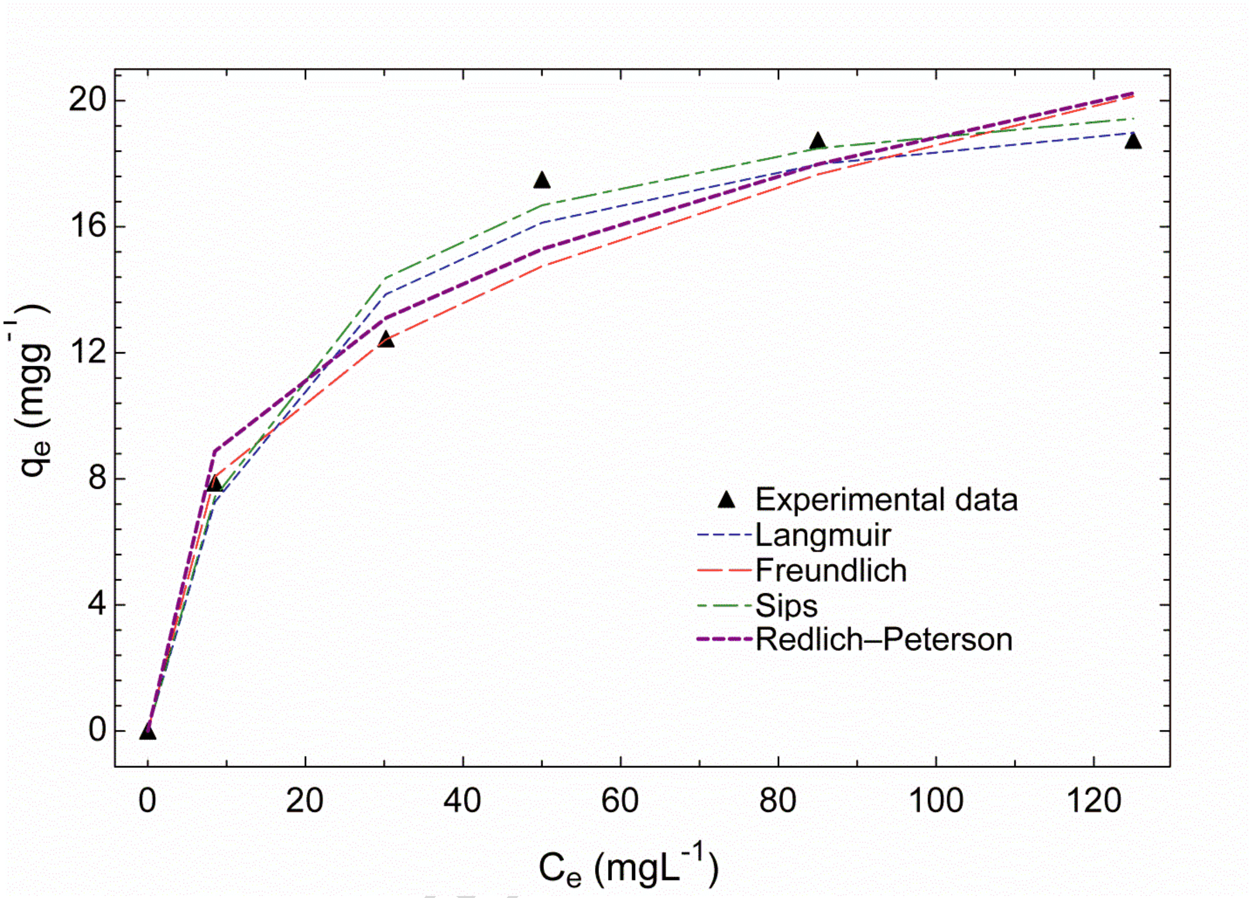

Fig. 9. Different isotherm models for nitrate adsorption by AC-2 (temperature=25° C, adsorbent dosage=0.2 g/50 mL, pH=7).

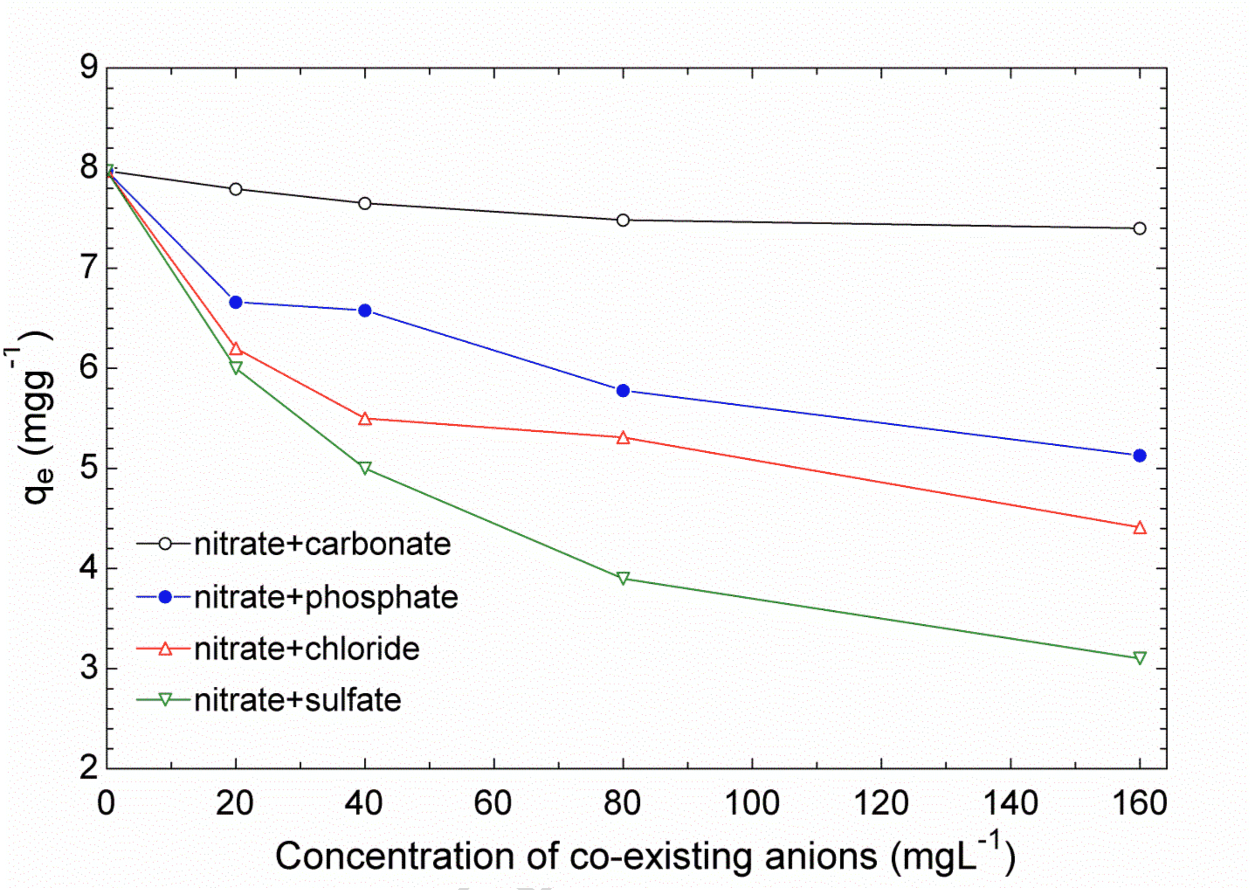

Fig. 10. Effects of presence other anions on nitrate adsorption capacity of AC-2 (temperature=25° C, adsorbent dosage=0.2 g/50 mL, pH=7, initial nitrate concentration=40 mgL^{-1}, initial co-existing anions=0-160 mgL^{-1}, contact time=120 min).

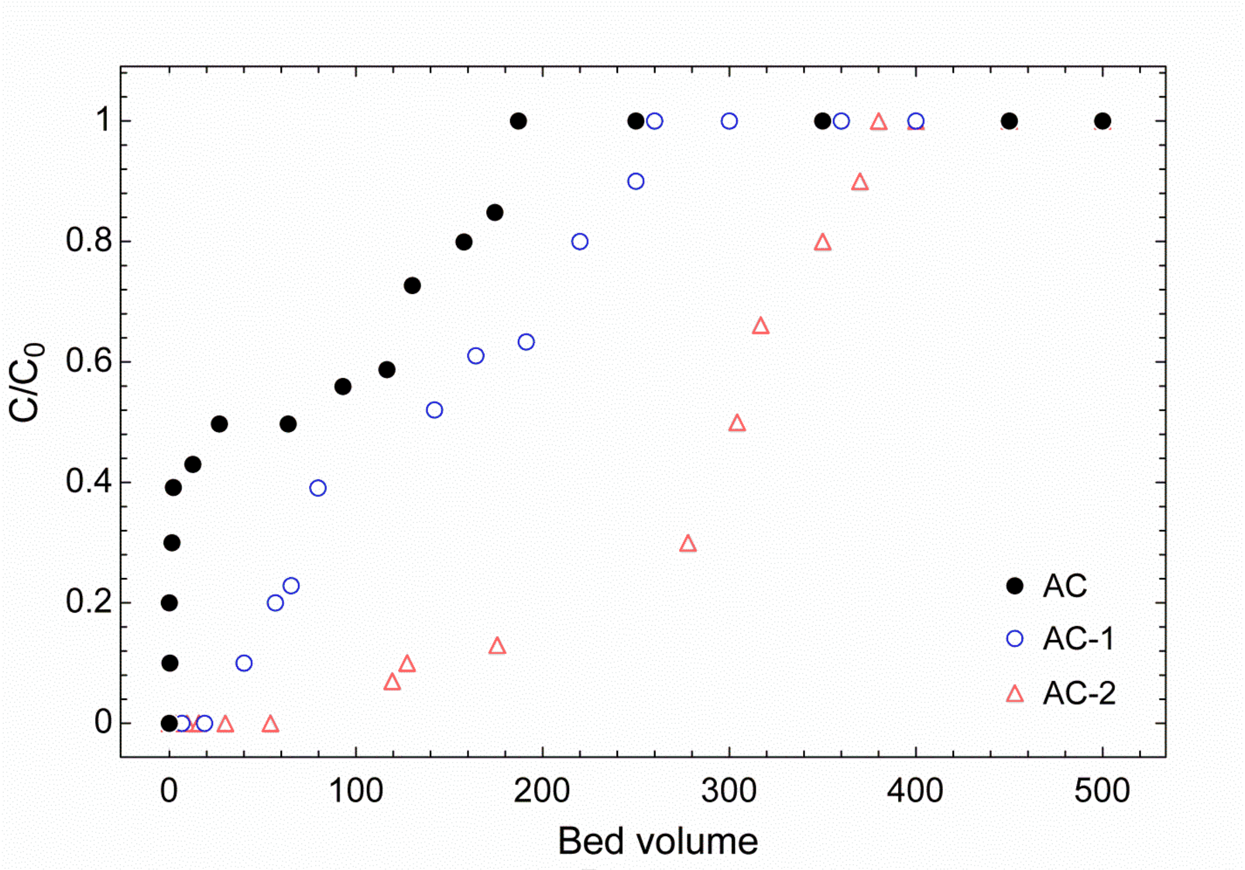

Fig. 11. Breakthrough curves of AC, AC-1, and AC-2 (initial concentration of NO_3^-=10 mg/L, temperature=25°C, flow reate= 2 mL/min, pH=7, empty bed contact time (EBCT)=9.5 min).

Table 1. Pore structure properties of activated carbons.

Adsorbents	S_{BET} (m^2g^{-1})	$V_{micro, DR}$ (cm^3g^{-1})	V_{total} (cm^3g^{-1})	V_{meso} (cm^3g^{-1})
AC	888	0.376	0.480	0.104
AC-1	901	0.400	0.490	0.090
AC-2	722	0.310	0.420	0.110

Table 2. Parameters of the pseudo-first-order, pseudo-second-order and intra-particle diffusion models for nitrate adsorbed by AC-2 (1 L solution, temperature=25° C, pH=7 and 4 g/L AC-2).

Model	Parameters	Unit	C_i=40 (mgL^{-1}) $(q_e)_{Exp.}$=8.00 (mgg^{-1})	C_i=80 (mgL^{-1}) $(q_e)_{Exp.}$=12.55 (mgg^{-1})
Pseudo-first-order	$(q_e)_{Cal.}$	mgg^{-1}	10.18	11.42
	k_1	min^{-1}	0.0244	0.0189
	R^2		0.98	0.97
	ARE		9.13	11.21
Pseudo-second-order	$(q_e)_{Cal.}$	mgg^{-1}	8.20	13.08
	k_2	gmg^{-1} min^{-1}	0.0022	0.0018
	R^2		0.99	0.99
	ARE		7.11	9.31
Intra-particle diffusion	k_{id}	mgg^{-1}min$^{-1/2}$	0.9412	1.007
	θ	mgg^{-1}	-1.4927	-0.9667
	R^2		0.99	0.97
	ARE		40.28	30.97

Table 3. Langmuir, Freundlich, Sips and Redlich-Peterson isotherm model parameters and correlation coefficient for adsorption of nitrate onto AC-2 (temperature=25° C, adsorbent dosage=0.2 g/50 mL, pH=7).

Adsorption isotherm	Parameters	Unit	Obtained value
Langmuir	q_m	(mgg^{-1})	21.51
	b	(Lmg^{-1})	0.06
	R_L		0.08-0.29
	R^2		0.99
	ARE		5.44
Freundlich	K_f	$(mgg^{-1})(Lmg^{-1})^{1/n}$	3.90
	n	(gL^{-1})	2.94
	R^2		0.94
	ARE		6.33
Sips	K_s	(Lmg^{-1})	0.055
	q_m	(mgg^{-1})	21.62
	n		0.95
	R^2		0.94
	ARE		6.18
Redlich-Peterson	K_R	Lg^{-1}	209.16
	α_R	Lmg^{-1}	45
	g		0.70
	R^2		0.90
	ARE		8.53

Table 4. Comparison of nitrate maximum adsorption capacity obtained in this work with previously reported ACs.

Adsorbents	q_m (mgg^{-1})	Concentration range (mgL^{-1})	Contact time	Temperature (˚C)	pH	Reference
AC derived from Pinus canariensis cones (PC-P)	9.92	6.2-496	-	25	2	[17]
PC-P thermally post-treated (PC-PT)	18.6					
PC-P post-treated with urea solution (PC-PU)	27.9					
Deashed F400 activated	13.5	100-800	24 h	25	5	[4]
F400 activated with ammonia at gas at 800°C	31.4					
Commercial AC Filtrasorb 400 (Cargon-Mitsubishi) (F400)	8.68	0-168	-	25	-	[5]
F400 oxidized with HNO_3 and outgassed at 800°C	8.06					
F400 oxidized with HNO_3 and outgassed at 1000°C	11.16					
F400 oxidized with HNO_3 and outgassed at 350°C (F400-Ox)						
•F400-Ox heat treated at 600°C	1.24					
•F400-Ox heat treated at 900°C	13.02					
- F400 activated with CO_2 at 900°C	7.44					
- F400 activated with steam at 1000°C	9.92					
Activated carbons developed with phosphoric acid (ACA)	6.82	6.2-372	-	25	2	[15]
Activated carbons developed with potassium hydroxide (ACB)	18.6					
Commercial activated carbon (ACC)	14.26					
Granular activated carbon made from lignite (Jarcarbon, Korea)	14.26	25.1-376	240 min	23±2	6.5-6.8	[21]
Cationic polymer-modified granular activated carbon (CPMG)	27.56					
Commercial AC Filtrasorb 400 (F400)	17.98	6.2-62	-	-	4	[57]
AC derived from sugar beet bagasse (activated under 700°C nitrogen flow by $ZnCl_2$	9.14 15.48	-	-	25 35	6.58	[51]

(impregnation ratio of 3:1)	27.55			45		
Wheat straw charcoal	1.10	0-25	10 min	15	-	[58]
Mustard straw charcoal	1.30					
Commercial activated carbon (Eureka Forbes Limited)	1.22					
AC derived from coconut shell	1.7	5-200	120 min	25	5.5	[14]
AC post-treated with $ZnCl_2$(impregnation ratio 200%) at 500°C air atmosphere furnace	10.2					
Impregnated almond shell activated carbon by Zn and $ZnSO_4$	16-17	10-50	120	20	6.2	[20]
Modified CACs	21.51	40-200	120 min	25	7	***This study***

Table 5. Thermodynamic parameters for the adsorption of nitrate on AC-2 at different temperatures.

Temperature (°C)	ΔG° (kJmol^{-1})	ΔH° (kJmol^{-1})	ΔS° (Jmol^{-1}K^{-1})
25	-17.10	-56.68	-132
35	-16.04		
45	-14.44		

Highlights

- Nitrate adsorption was studied onto modified activated carbons (AC).
- Maximum adsorption capacity of modified AC for nitrate was 21.51 mg g^{-1}.
- The breakthrough point of AC-2 was 54 bed volumes in the column study.